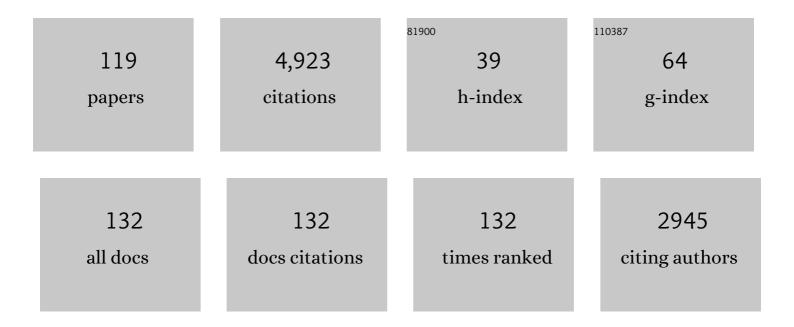
List of Publications by Year in descending order

Source: https://exaly.com/author-pdf/7953383/publications.pdf Version: 2024-02-01



NIKIASLINDE

#	Article	IF	CITATIONS
1	Lasting Effects of Soil Compaction on Soil Water Regime Confirmed by Geoelectrical Monitoring. Water Resources Research, 2022, 58, e2021WR030696.	4.2	6
2	Simulating Fullyâ€Integrated Hydrological Dynamics in Complex Alpine Headwaters: Potential and Challenges. Water Resources Research, 2022, 58, .	4.2	12
3	Hydrogeological multiple-point statistics inversion by adaptive sequential Monte Carlo. Advances in Water Resources, 2022, 166, 104252.	3.8	3
4	Bayesian tomography with prior-knowledge-based parametrization and surrogate modelling. Geophysical Journal International, 2022, 231, 673-691.	2.4	5
5	Adaptive sequential Monte Carlo for posterior inference and model selection among complex geological priors. Geophysical Journal International, 2021, 226, 1220-1238.	2.4	6
6	Approaching geoscientific inverse problems with vector-to-image domain transfer networks. Advances in Water Resources, 2021, 152, 103917.	3.8	8
7	Seismic signatures reveal persistence of soil compaction. Vadose Zone Journal, 2021, 20, e20140.	2.2	11
8	Individual and joint inversion of head and flux data by geostatistical hydraulic tomography. Advances in Water Resources, 2021, 154, 103960.	3.8	5
9	Lithological tomography with the correlated pseudo-marginal method. Geophysical Journal International, 2021, 228, 839-856.	2.4	4
10	Using deep generative neural networks to account for model errors in Markov chain Monte Carlo inversion. Geophysical Journal International, 2021, 228, 1098-1118.	2.4	6
11	Heat transport by flow through rough rock fractures: a numerical investigation. Advances in Water Resources, 2021, 156, 104042.	3.8	11
12	GPR-inferred fracture aperture widening in response to a high-pressure tracer injection test at the Äspö Hard Rock Laboratory, Sweden. Engineering Geology, 2021, 292, 106249.	6.3	3
13	Inferring geostatistical properties of hydraulic conductivity fields from saline tracer tests and equivalent electrical conductivity time-series. Advances in Water Resources, 2020, 146, 103758.	3.8	4
14	Which fractures are imaged with Ground Penetrating Radar? Results from an experiment in the Äspö Hardrock Laboratory, Sweden. Engineering Geology, 2020, 273, 105674.	6.3	13
15	Advancing quantitative understanding of self-potential signatures in the critical zone through long-term monitoring. Journal of Hydrology, 2020, 585, 124771.	5.4	16
16	Time-Lapse Seismic and Electrical Monitoring of the Vadose Zone during a Controlled Infiltration Experiment at the Ploemeur Hydrological Observatory, France. Water (Switzerland), 2020, 12, 1230.	2.7	19
17	Time-lapse cross-hole electrical resistivity tomography (CHERT) for monitoring seawater intrusion dynamics in a Mediterranean aquifer. Hydrology and Earth System Sciences, 2020, 24, 2121-2139.	4.9	45
18	Hydrogeological Model Selection Among Complex Spatial Priors. Water Resources Research, 2019, 55, 6729-6753.	4.2	14

#	Article	IF	CITATIONS
19	Joint probabilistic inversion of DC resistivity and seismic refraction data applied to bedrock/regolith interface delineation. Journal of Applied Geophysics, 2019, 170, 103839.	2.1	13
20	Gradient-based deterministic inversion of geophysical data with generative adversarial networks: Is it feasible?. Computers and Geosciences, 2019, 133, 104333.	4.2	41
21	Bayesian Inference of Subglacial Channel Structures From Water Pressure and Tracerâ€Transit Time Data: A Numerical Study Based on a 2â€D Geostatistical Modeling Approach. Journal of Geophysical Research F: Earth Surface, 2019, 124, 1625-1644.	2.8	6
22	Bayesian full-waveform tomography with application to crosshole ground penetrating radar data. Geophysical Journal International, 2019, 218, 913-931.	2.4	17
23	Simulation of fine-scale electrical conductivity fields using resolution-limited tomograms and area-to-point kriging. Geophysical Journal International, 2019, 218, 1322-1335.	2.4	9
24	Reduction of conceptual model uncertainty using ground-penetrating radar profiles: Field-demonstration for a braided-river aquifer. Journal of Hydrology, 2019, 571, 254-264.	5.4	8
25	The buried caldera boundary of the Vesuvius 1631 eruption revealed by present-day soil CO2 concentration. Journal of Volcanology and Geothermal Research, 2019, 375, 43-56.	2.1	2
26	Trainingâ€Image Based Geostatistical Inversion Using a Spatial Generative Adversarial Neural Network. Water Resources Research, 2018, 54, 381-406.	4.2	232
27	Impact of small-scale saline tracer heterogeneity on electrical resistivity monitoring in fully and partially saturated porous media: Insights from geoelectrical milli-fluidic experiments. Advances in Water Resources, 2018, 113, 295-309.	3.8	28
28	Impact of petrophysical uncertainty on Bayesian hydrogeophysical inversion and model selection. Advances in Water Resources, 2018, 111, 346-359.	3.8	21
29	Geoelectrical Signatures of Reactive Mixing: A Theoretical Assessment. Geophysical Research Letters, 2018, 45, 3489-3498.	4.0	6
30	Probabilistic inference of fracture-scale flow paths and aperture distribution from hydrogeophysically-monitored tracer tests. Journal of Hydrology, 2018, 567, 305-319.	5.4	8
31	A Review of Geophysical Methods for Soil Structure Characterization. Reviews of Geophysics, 2018, 56, 672-697.	23.0	97
32	A Quantitative Comparison of GPR Sections to Reduce Geological Prior Uncertainty. , 2018, , .		0
33	Probabilistic inversion with graph cuts: Application to the <scp>B</scp> oise <scp>H</scp> ydrogeophysical <scp>R</scp> esearch <scp>S</scp> ite. Water Resources Research, 2017, 53, 1231-1250.	4.2	15
34	Bayesian model selection in hydrogeophysics: Application to conceptual subsurface models of the South Oyster Bacterial Transport Site, Virginia, USA. Advances in Water Resources, 2017, 102, 127-141.	3.8	30
35	Neutrally buoyant tracers in hydrogeophysics: Field demonstration in fractured rock. Geophysical Research Letters, 2017, 44, 3663-3671.	4.0	14
36	Longâ€Term Soil Structure Observatory for Monitoring Postâ€Compaction Evolution of Soil Structure. Vadose Zone Journal, 2017, 16, 1-16.	2.2	63

#	Article	IF	CITATIONS
37	Pore network modeling of the electrical signature of solute transport in dualâ€domain media. Geophysical Research Letters, 2017, 44, 4908-4916.	4.0	25
38	Inference of multi-Gaussian relative permittivity fields by probabilistic inversion of crosshole ground-penetrating radar data. Geophysics, 2017, 82, H25-H40.	2.6	11
39	On structure-based priors in Bayesian geophysical inversion. Geophysical Journal International, 2017, 208, 1342-1358.	2.4	12
40	Inversion using a new low-dimensional representation of complex binary geological media based on a deep neural network. Advances in Water Resources, 2017, 110, 387-405.	3.8	155
41	On uncertainty quantification in hydrogeology and hydrogeophysics. Advances in Water Resources, 2017, 110, 166-181.	3.8	82
42	The 3-D structure of the Somma-Vesuvius volcanic complex (Italy) inferred from new and historic gravimetric data. Scientific Reports, 2017, 7, 8434.	3.3	18
43	Apparent apertures from ground penetrating radar data and their relation to heterogeneous aperture fields. Geophysical Journal International, 2017, 209, 1418-1430.	2.4	16
44	GEOELECTRICAL MONITORING OF SOLUTE TRANSPORT IN DUAL-DOMAIN MEDIA: A REVIEW. , 2017, , .		1
45	Patchâ€based iterative conditional geostatistical simulation using graph cuts. Water Resources Research, 2016, 52, 6297-6320.	4.2	30
46	Hydrogeophysical characterization of transport processes in fractured rock by combining pushâ€pull and singleâ€hole ground penetrating radar experiments. Water Resources Research, 2016, 52, 938-953.	4.2	30
47	Streaming potential modeling in fractured rock: Insights into the identification of hydraulically active fractures. Geophysical Research Letters, 2016, 43, 4937-4944.	4.0	33
48	Merging parallel tempering with sequential geostatistical resampling for improved posterior exploration of high-dimensional subsurface categorical fields. Advances in Water Resources, 2016, 90, 57-69.	3.8	28
49	Image synthesis with graph cuts: a fast model proposal mechanism in probabilistic inversion. Geophysical Journal International, 2016, 204, 1179-1190.	2.4	38
50	Electrical Resistivity Monitoring of Saline Tracer Fingering at Pore Scale under Partially Saturated Conditions. , 2016, , .		2
51	Tomogram-based comparison of geostatistical models: Application to the Macrodispersion Experiment (MADE) site. Journal of Hydrology, 2015, 531, 543-556.	5.4	13
52	Probabilistic inference of multiâ€ <scp>G</scp> aussian fields from indirect hydrological data using circulant embedding and dimensionality reduction. Water Resources Research, 2015, 51, 4224-4243.	4.2	39
53	Monitoring of saline tracer movement with vertically distributed self-potential measurements at the HOBE agricultural test site, Voulund, Denmark. Journal of Hydrology, 2015, 521, 314-327.	5.4	57
54	Summary statistics from training images as prior information in probabilistic inversion. Geophysical Journal International, 2015, 201, 157-171.	2.4	46

#	Article	IF	CITATIONS
55	Feature-preserving interpolation and filtering of environmental time series. Environmental Modelling and Software, 2015, 72, 71-76.	4.5	10
56	Effective modeling of ground penetrating radar in fractured media using analytic solutions for propagation, thin-bed interaction and dipolar scattering. Journal of Applied Geophysics, 2015, 116, 206-214.	2.1	17
57	An analytical study of seismoelectric signals produced by 1-D mesoscopic heterogeneities. Geophysical Journal International, 2015, 201, 329-342.	2.4	13
58	Geological realism in hydrogeological and geophysical inverse modeling: A review. Advances in Water Resources, 2015, 86, 86-101.	3.8	152
59	Probabilistic 3-D time-lapse inversion of magnetotelluric data: application to an enhanced geothermal system. Geophysical Journal International, 2015, 203, 1946-1960.	2.4	33
60	Morphological, hydrological, biogeochemical and ecological changes and challenges in river restoration – the Thur River case study. Hydrology and Earth System Sciences, 2014, 18, 2449-2462.	4.9	46
61	Falsification and corroboration of conceptual hydrological models using geophysical data. Wiley Interdisciplinary Reviews: Water, 2014, 1, 151-171.	6.5	16
62	Conditioning of Multiple-Point Statistics Facies Simulations to Tomographic Images. Mathematical Geosciences, 2014, 46, 625-645.	2.4	28
63	3-D density structure and geological evolution of Stromboli volcano (Aeolian Islands, Italy) inferred from land-based and sea-surface gravity data. Journal of Volcanology and Geothermal Research, 2014, 273, 58-69.	2.1	17
64	Two-dimensional probabilistic inversion of plane-wave electromagnetic data: methodology, model constraints and joint inversion with electrical resistivity data. Geophysical Journal International, 2014, 196, 1508-1524.	2.4	60
65	Probabilistic electrical resistivity tomography of a CO2 sequestration analog. Journal of Applied Geophysics, 2014, 107, 80-92.	2.1	30
66	Conditioning of stochastic 3-D fracture networks to hydrological and geophysical data. Advances in Water Resources, 2013, 62, 79-89.	3.8	46
67	Distributed Soil Moisture from Crosshole Groundâ€Penetrating Radar Travel Times using Stochastic Inversion. Vadose Zone Journal, 2013, 12, 1-16.	2.2	47
68	Structure-coupled joint inversion of geophysical and hydrological data. Geophysics, 2013, 78, ID1-ID14.	2.6	39
69	3-D characterization of high-permeability zones in a gravel aquifer using 2-D crosshole GPR full-waveform inversion and waveguide detection. Geophysical Journal International, 2013, 195, 932-944.	2.4	76
70	3D characterization of an aquifer using full-waveform inversion and amplitude analysis. , 2013, , .		0
71	Selfâ€Potentials in Partially Saturated Media: The Importance of Explicit Modeling of Electrode Effects. Vadose Zone Journal, 2013, 12, 1-21.	2.2	36
72	Seismoelectric effects due to mesoscopic heterogeneities. Geophysical Research Letters, 2013, 40, 2033-2037.	4.0	35

#	Article	IF	CITATIONS
73	Imaging and quantifying salt-tracer transport in a riparian groundwater system by means of 3D ERT monitoring. Geophysics, 2012, 77, B207-B218.	2.6	83
74	Estimating traveltimes and groundwater flow patterns using 3D time-lapse crosshole ERT imaging of electrical resistivity fluctuations induced by infiltrating river water. Geophysics, 2012, 77, E239-E250.	2.6	49
75	Fracture imaging within a granitic rock aquifer using multiple-offset single-hole and cross-hole GPR reflection data. Journal of Applied Geophysics, 2012, 78, 123-132.	2.1	43
76	Constraining 3-D electrical resistance tomography with GPR reflection data for improved aquifer characterization. Journal of Applied Geophysics, 2012, 78, 68-76.	2.1	100
77	A filtering method to correct time-lapse 3D ERT data and improve imaging of natural aquifer dynamics. Journal of Applied Geophysics, 2012, 80, 12-24.	2.1	15
78	Focused time-lapse inversion of radio and audio magnetotelluric data. Journal of Applied Geophysics, 2012, 84, 29-38.	2.1	26
79	Inferring transport characteristics in a fractured rock aquifer by combining singleâ€hole groundâ€penetrating radar reflection monitoring and tracer test data. Water Resources Research, 2012, 48, .	4.2	40
80	Derivation of Soilâ€Specific Streaming Potential Electrical Parameters from Hydrodynamic Characteristics of Partially Saturated Soils. Vadose Zone Journal, 2012, 11, .	2.2	95
81	Mass conservative threeâ€dimensional water tracer distribution from Markov chain Monte Carlo inversion of timeâ€lapse groundâ€penetrating radar data. Water Resources Research, 2012, 48, .	4.2	45
82	Single-hole GPR reflection imaging of solute transport in a granitic aquifer. Geophysical Research Letters, 2011, 38, n/a-n/a.	4.0	35
83	Hydrogeophysics. , 2011, , 401-434.		35
84	Towards improved instrumentation for assessing river-groundwater interactions in a restored river corridor. Hydrology and Earth System Sciences, 2011, 15, 2531-2549.	4.9	47
85	Self-potential investigations of a gravel bar in a restored river corridor. Hydrology and Earth System Sciences, 2011, 15, 729-742.	4.9	32
86	Comment on â€~Streaming potential dependence on water-content in Fontainebleau sand' by V. AllÔgre, L. Jouniaux, F. Lehmann and P. Sailhac. Geophysical Journal International, 2011, 186, 113-114.	2.4	9
87	3D crosshole ERT for aquifer characterization and monitoring of infiltrating river water. Geophysics, 2011, 76, G49-G59.	2.6	100
88	High resolution imaging of the unsaturated and saturated zones of a gravel aquifer using full-waveform inversion. , 2011, , .		4
89	Fullâ€waveform inversion of crossâ€hole groundâ€penetrating radar data to characterize a gravel aquifer close to the Thur River, Switzerland. Near Surface Geophysics, 2010, 8, 635-649.	1.2	92
90	Full-waveform inversion of crosshole ground penetrating radar data to characterize a gravel aquifer close to the Thur River, Switzerland. , 2010, , .		15

IF # ARTICLE CITATIONS The borehole-fluid effect in electrical resistivity imaging. Geophysics, 2010, 75, F107-F114. 1. Joint Inversion of Crosshole GPR and Seismic Traveltime Data., 2010, , 1-16. 92 8 Structural joint inversion of timeâ€lapse crosshole ERT and GPR traveltime data. Geophysical Research 4.0 Letters, 2010, 37, . Zonation for 3D aquifer characterization based on joint inversions of multimethod crosshole 94 2.6 134 geophysical data. Geophysics, 2010, 75, G53-G64. A Multi-borehole 3-D ERT Monitoring System for Aquifer Characterization Using River Flood Events as a Natural Tracer., 2010,,. 96 Critical Steps for the Continuing Advancement of Hydrogeophysics. Eos, 2009, 90, 200-200. 0.1 60 Comment on "Characterization of multiphase electrokinetic coupling using a bundle of capillary 3.3 tubes model―by Mathew D. Jackson. Journal of Geophysical Research, 2009, 114, . Redox potential distribution inferred from selfâ€potential measurements associated with the 98 1.9 64 corrosion of a burden metallic body. Geophysical Prospecting, 2008, 56, 269-282. Detection and localization of hydromechanical disturbances in a sandbox using the selfa \in potential 3.3 method. Journal of Geophysical Research, 2008, 113, . Joint inversion of crosshole radar and seismic traveltimes acquired at the South Oyster Bacterial 100 2.6 78 Transport Site. Geophysics, 2008, 73, G29-G37. Experimental Design for Crosshole Electrical Resistivity Tomography Data Sets., 2008, , . A comment on $\hat{a} \in \infty$ Electrical tomography of La Soufri \tilde{A} re of Guadeloupe Volcano: Field experiments, 1D inversion and qualitative interpretationâé•by Nicollin, F. et al. [Earth Planet. Sci. Lett. 244 (2006) 102 4.4 6 709–724]. Earth and Planetary Science Letters, 2007, 258, 619-622. Estimation of the water table throughout a catchment using self-potential and piezometric data in a 5.4 Bayesian framework. Journal of Hydrology, 2007, 334, 88-98. Streaming current generation in two-phase flow conditions. Geophysical Research Letters, 2007, 34, . 104 4.0 122 Inverting selfâ€potential data for redox potentials of contaminant plumes. Geophysical Research Letters, 2007, 34, . Electrokinetic coupling in unsaturated porous media. Journal of Colloid and Interface Science, 2007, 106 9.4 205 313, 315-327. Non-intrusive characterization of the redox potential of landfill leachate plumes from self-potential 3.3 data. Journal of Contaminant Hydrology, 2007, 92, 274-292. 108 Inversion of tracer test data using tomographic constraints. Water Resources Research, 2006, 42, . 4.2 64

NIKLAS LINDE

#	Article	IF	CITATIONS
109	Local earthquake (LE) tomography with joint inversion for P- and S-wave velocities using structural constraints. Geophysical Research Letters, 2006, 33, .	4.0	59
110	Improved hydrogeophysical characterization using joint inversion of cross-hole electrical resistance and ground-penetrating radar traveltime data. Water Resources Research, 2006, 42, .	4.2	270
111	Chemico-electromechanical coupling in microporous media. Journal of Colloid and Interface Science, 2006, 302, 682-694.	9.4	172
112	HYDROGEOPHYSICAL PARAMETER ESTIMATION APPROACHES FOR FIELD SCALE CHARACTERIZATION. , 2006, , 9-44.		18
113	Evidence of electrical anisotropy in limestone formations using the RMT technique. Geophysics, 2004, 69, 909-916.	2.6	36
114	Chemical denudation in arctic-alpine Latnjavagge (Swedish Lapland) in relation to regolith as assessed by radio magnetotelluric-geophysical profiles. Geomorphology, 2004, 57, 303-319.	2.6	50
115	Characterization of a fractured granite using radio magnetotelluric (RMT) data. Geophysics, 2004, 69, 1155-1165.	2.6	29
116	Assessment of chemical denudation rates using hydrological measurements, water chemistry analysis and electromagnetic geophysical data. Permafrost and Periglacial Processes, 2003, 14, 387-397.	3.4	21
117	Multicriteria Decision Aid in Supporting Decisions Related to Groundwater Protection. Environmental Management, 2003, 32, 589-601.	2.7	11
118	Probabilistic inference of subsurface heterogeneity and interface geometry using geophysical data. Geophysical Journal International, 0, , .	2.4	10
119	Electrical Signatures of Diffusion-Limited Mixing: Insights from a Milli-fluidic Tracer Experiment.	2.6	2